

Quantum tunneling in nanomagnetic systems with different uniaxial anisotropy order

This article has been downloaded from IOPscience. Please scroll down to see the full text article.

2009 Nanotechnology 20 465403

(<http://iopscience.iop.org/0957-4484/20/46/465403>)

[The Table of Contents](#) and [more related content](#) is available

Download details:

IP Address: 200.1.18.60

The article was downloaded on 22/10/2009 at 14:51

Please note that [terms and conditions apply](#).

Quantum tunneling in nanomagnetic systems with different uniaxial anisotropy order

J M Florez¹, Álvaro S Núñez² and P Vargas¹

¹ Departamento de Física, Universidad Técnica Federico Santa María, PO Box 110-V, Valparaíso, Chile

² Departamento de Física, Facultad de Ciencias Físicas y Matemáticas, Universidad de Chile, Casilla 487-3, Santiago, Chile

E-mail: juanmanuel.florez@postgrado.usm.cl

Received 9 June 2009, in final form 1 October 2009

Published 22 October 2009

Online at stacks.iop.org/Nano/20/465403

Abstract

A study of macroscopic quantum tunneling (MQT) of the magnetic moment in systems with quadratic and higher order uniaxial anisotropy and Zeeman interaction is presented. By using the instanton technique, under the giant spin approximation, the escape rate or probability per unit of time Γ that the system undergoes a transition between coherent or metastable states is calculated. Using an effective particle potential we also determine the escape temperature $T_c(T)$, which marks the transition from quantum tunneling to thermal activation. A discussion is presented about the different models and the behavior of the magnetic system under the tunneling regime.

(Some figures in this article are in colour only in the electronic version)

1. Introduction

Study of the dynamics of molecular nanomagnets (MNM) has attracted great interest from scientists due to both its fundamental significance in the context of quantum dynamics and its potential applications in the context of information processing and storage. Of the basic phenomena associated with MNM dynamics, a great variety can be accounted for in terms of a simple qualitative picture provided by the giant spin model.

The study of macroscopic quantum tunneling (MQT) in magnetic systems began around two decades ago [1, 2]. In general the problem of estimating the transition amplitude A or escape rate Γ ($\Gamma \propto |A|^2$) between any two metastable states associated with a Hamiltonian \hat{H} has been addressed from two complementary points of view. For simple enough systems, we can perform full diagonalization of the Hamiltonian to find out the eigenstates. On the other hand, the amplitude can be regarded as the imaginary-time ($\tau = it$) path integral

$$\int \mathcal{D}[\Omega(\tau)] e^{-\frac{I_\xi}{\hbar}} \quad (1)$$

where $I_\xi = \int d\tau (-L_E)$ with $L_E = L_{cl}(-i\tau)$ (classical Lagrangian) is the Euclidean action. To estimate the amplitude,

the steepest descent method is used, where paths of minimum action are considered to dominate evaluation. Such paths are called instantons.

As part of MQT studies in nanomagnetic systems, quantum tunneling of domain walls and quantum nucleation have been studied within the realm of validity of the instanton technique [1, 3–7]. On the other hand, despite difficulty in generating arrangements of isolated nanosystems, several experiments have proved the presence of tunneling in different systems [1, 6, 8–11]. Those results can be explained by modeling the magnetic relaxation process with a magnetic viscosity that depends strongly on Γ . The plateau that viscosity exhibits is understood by analyzing the behavior of Γ at low temperature. Where the plateaus are present on the magnetic hysteresis curves another approach known as the Landau–Zener (LZ) theory has been widely used to determine the tunneling probability [12–15]. The Lagrangian applied to the giant spin framework (equation (1)) can represent an effective molecular spin or a magnetic particle, which at a macroscopic level shows a tunneling process. The observation of such tunneling depends on magnetic field separation of the steps in magnetization, among other things. It has been shown that in tunneling of the noncompensated spin

in some antiferromagnetic nanoparticles, this separation of steps is comparable with the step separation for the Mn_{12} molecule. Even in the case of simultaneous collective resonance only to zero magnetic field, magnetic relaxation presents a characteristic peak in the magnetic viscosity when the temperature increases, and which is due to thermally assisted tunneling [9].

In this work we focus on studying the tunneling of giant spins between states separated by an intermediate metastable state. The presence of such a state is ensured by modification of the anisotropy contributions of the magnetic Hamiltonian. The calculation is performed from two independent viewpoints. In the first we find the periodic instanton trajectories which minimize the Euclidean action for the Hamiltonian density \mathcal{H} in equation (2) and then we calculate equation (1) by using the steepest descent method. In the second method we use mapping to find an effective action in order to obtain a unidimensional particle equation of movement. Then we find the escape exponent I_{ξ} by using the period of the instantons as a function of energy.

In order to address the problem, we consider a single magnetic moment in an external field, with a higher-order magnetic anisotropy. Studies of spin reversal for quadratic biaxial and uniaxial anisotropy with fourth-order contributions have been presented within the instanton formalism, perturbative theory, and LZ theory among others [16–22]—at present we do not know of any reports on the escape rate for \mathcal{H} with higher-order uniaxial magnetic anisotropy and under a transverse Zeeman interaction. Therefore, in this work we use the instanton formalism to calculate this latter case and take into account not only quadratic anisotropy terms but also contributions of the fourth-order anisotropy term. Moreover, we calculate the escape exponent in Γ , and the escape temperature $T_c(\beta^{-1})$ characterizing the crossing from thermally assisted quantum tunneling to classical thermal activation. These factors are calculated within the effective particle model and for the case of quadratic anisotropy where an exact mapping has been possible [23–29].

The importance of the escape exponent lies in the general dependence of Γ on this simple term. Even when quantum fluctuations are taken into account the factor $\exp(-I_{\xi}/\hbar)$ appears as fundamental in the final expression for Γ . In most cases this exponential factor dominates the behavior of the tunneling rate. In fact, when the tunneling is affected by the contributions of different excited levels [30, 31], an Arrhenius-like behavior persists on the dynamical description for MNMs which also occurs up to quartic anisotropy terms [31]. Additionally, the topological oscillations of the energy splitting for the magnetic molecule of Fe_8 can be explained just with the inclusion of fourth-order terms in the spin Hamiltonian [13, 18].

The present work is structured as follows. In section 2.1 a basic model that displays the continuous appearance of a metastable state between two globally stable or coherent states is presented. The effects of such a state over the tunneling rates and the extent of the modifications it mediates on the methods used as well as their range of validity are discussed

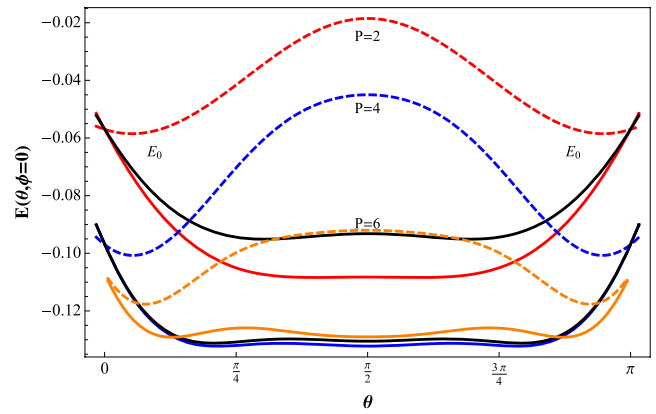


Figure 1. Energy landscapes provided by equation (2) considering κ_2 and $P = 2$ (red), κ_2 and $P = 4$ (blue), κ_2 and $P = 6$ (orange), $M = 10$ and magnetic field for two illustrative values $H_{\text{ext}} = ((0.00975, 0.05697), (0.00921, 0.01285))$ correspondingly. The black lines are for $P = 2, 4$ with fields $H_{\text{ext}} = 0.04905$ (between dashed lines for $P = 4$ (up) and $P = 6$ (down)), 0.01306 (between continuous lines for $P = 6$ (up) and $P = 4$ (down)). $\kappa_2 = 0.114$ meV and $\kappa_4 = 0.16$ meV, and $\kappa_6 = 0.3$ meV E_0 indicates the position of the more stable minima.

in sections 2.2 and 4. In section 3.1 we discuss two different models to map \mathcal{H} for $P = 2$ to a reduced action I_{ξ} . Then this is calculated throughout an integral function which we propose. The rates as a function of H_{ext} and $T_c(T)$ are considered in 3.2 and a general discussion is provided in 4.

2. Magnetic tunneling: instantons for Euclidean action

In this section we introduce the model and highlight its main features. Simple tunneling rate calculations are then described and their physical content discussed. Finally a brief discussion of the relevance of the results is presented.

2.1. Basic model

Our study is based on a modified macrospin Hamiltonian. The essential change is the incorporation of a higher-order of the energy dependence on the magnetization projection along the easy axis z . This modification introduces a local minimum around $\theta = \pi/2$, while keeping the minima corresponding to coherent or stable states:

$$\mathcal{H} = -\left(\frac{\kappa_2}{2}\Omega_z^2 + \frac{\kappa_P}{P}\Omega_z^P\right) - H_{\text{ext}}M\Omega_x. \quad (2)$$

Here H_{ext} is an external magnetic field along axis x , M is the magnitude of the magnetic moment, while Ω represents the unitary vector along the magnetic moment. κ_2 and κ_P represent the second- and P -order uniaxial energy constants. The uniaxial anisotropy is taken along the z -axis. (Throughout the paper we use $\hbar = \gamma = g\mu_B/\hbar = 1$ for calculations.)

A quick look at equation (2) shows a local minimum located right at $\pi/2$ and therefore between the two degenerated local minima E_0 for $P > 2$. This state is metastable as long as $H_{\text{ext}} > \kappa_2$. In this way by adjusting the external field strength we can induce the presence of an intermediate state figure 1 that will prove effective in changing the tunneling rates. This

is the essential feature of the simple model that more realistic models share.

The analysis of the tunneling properties can focus on studying the escape temperature. The escape temperature, which is [1] $T_e(T) \approx \Delta U_o/I_\xi(T)$ (where ΔU_o is the height of the barrier between two minimum states), can be naturally associated, under appropriate environmental circumstances, with the magnetic viscosity in the tunneling regime. It can be used to describe the transition from a thermally assisted quantum tunneling regime toward the classical Kramers-like [32–34] regime. The nature of this system shows us how the magnetic field modifies the metastable state. Thus, we calculate instantons for lower energies compared to ΔU_o as well as escape exponents as a function of temperature.

2.2. Instanton calculations

The problem is then reduced to finding the paths that minimize the exponent in equation (1) and to evaluating the Euclidean action along these. These can be evaluated from the classical action I_{cl} , as follows:

$$I_{cl} = \int dt \left(\frac{M}{\gamma} \dot{\phi} (\cos \theta - 1) - E(\theta, \phi) \right) \quad (3)$$

where $E(\theta, \phi)$ is the energy function of equation (2). From the motion equations, we can directly obtain (using $\omega_H = \gamma H_{ext}$, $\omega_1 = \frac{\gamma \kappa_2}{M}$, $\omega_P = \frac{\gamma \kappa_P}{M}$):

$$\ddot{\theta}(\tau) = \left[\omega_P (\cos \theta)^{P-2} - \omega_H \frac{G(\dot{\theta})}{\sin \theta} + \omega_1 \right] \omega_H G(\dot{\theta}) \cos \theta \quad (4)$$

where $G(\dot{\theta})$ is

$$G(\dot{\theta}(\tau)) = \sqrt{1 + \left(\frac{\dot{\theta}(\tau)}{\omega_H} \right)^2} \quad (5)$$

The solution of that equation can be found in a straightforward calculation. The final Euclidean action I_ξ of equation (1) which determines the escape rate is obtained from the periodic instanton solution by using equations (4) and (5). In figure 2 we present instanton trajectories, $\theta(\tau)$, for 20 different values of the external field. Every black line indicates a different external magnetic field within the interval indicated in the caption. The effects of the metastable state clearly show the appearance of a kink near $\theta \approx \pi/2$. This kink naturally has the effect of extending the period of the instanton trajectory. This can be seen, for each case, in the corresponding return points marked in the figures. The $P = 2$ case in figure 2 indicates the case when only κ_2 is considered. Therefore, the effect is that the instanton tends to remain longer near $\theta \approx \pi/2$.

In figure 3 we show the escape exponent I_ξ for instantons (upper panel) with $P = 2$, corresponding to what is shown in figure 2 and the corresponding escape temperature (lower panel). Figure 4 depicts the escape exponent and temperature for the case of $P = 4$. The Arrhenius-like exponent in the graphics measures, within the realm of Kramers theory, the over-barrier thermal activation between the initial coherent state and the metastable state. We also found the solutions for the instantons and the escape rate for the case $P = 6$ (not shown here), although it is possible to find more than one minimum between the stable states for some parameters.

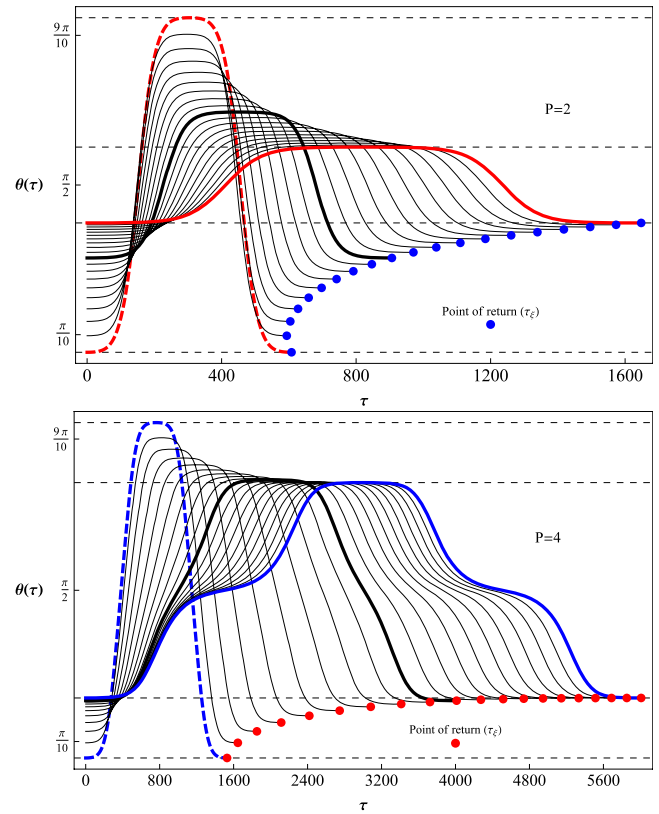


Figure 2. Magnetic instanton solutions for equations (4) and (5) with $\omega_1 = 0.01$, $\omega_{P=2} = 0.05$, $\omega_{P=4} = 0.016$, $M = 10$ and an external magnetic field corresponding to H_{ext} = (red-dashed line, black-thick line, red-thick line) = (0.009 75, 0.049 05, 0.056 97) for $P = 2$ and H_{ext} = (blue-dashed line, black-thick line, blue-thick line) = (0.004 69, 0.013 05, 0.013 23) for $P = 4$. The other black lines are for an external magnetic field which ranges between the above values. The step field used follows a simple function $H(i)_{ext} = H_o(1 - \mathcal{F}(i))$, where $\mathcal{F}(i) = (1/H_d/H_d) \dots i \text{ times} \dots /H_d$ and $(H_o = 0.0585, 0.0132, H_d = 1.2, 1.55)$ for $P = 2, 4$, respectively. The constant dashed lines show the values of θ among which the instantons oscillate for some energy close to the minimum as $\Delta U_o/10^4$. The dashed-thick line represents the lower field and the continuous line the bigger magnetic field. The exact points where the instantons return for the graphics without these constant lines are marked with blue and red points for $P = 2, 4$, respectively.

3. Instantons for effective particle potential

3.1. Mapping into a reduced action

In this section we introduce a formal mapping method that improves upon the methods described in the previous section [23–27]. Using the canonical representation $P_\theta = S \cos \theta$ and $X_\phi = \dot{\phi}$ we can transform the Hamiltonian into the form $P_\theta^2/2m(\phi) + V_{ef}(\phi)$, where $m(\phi)$ is a functional mass containing the inertial momentum for rotation under the barrier and $V_{ef}(\phi)$ is the new effective potential. The canonically conjugated pair of variables used here justifies the choice to obtain the classical equations of motion from the Lagrangian $\mathbf{L} = P_\theta \dot{X}_\phi - \hat{H}$ (with \hat{H} in the large spin approximation). This method is a powerful one, as the dependence on θ in that potential can be included exactly in P_θ [23–25]. In our case the presence of terms with $\kappa_P \neq 0$ could be accounted for

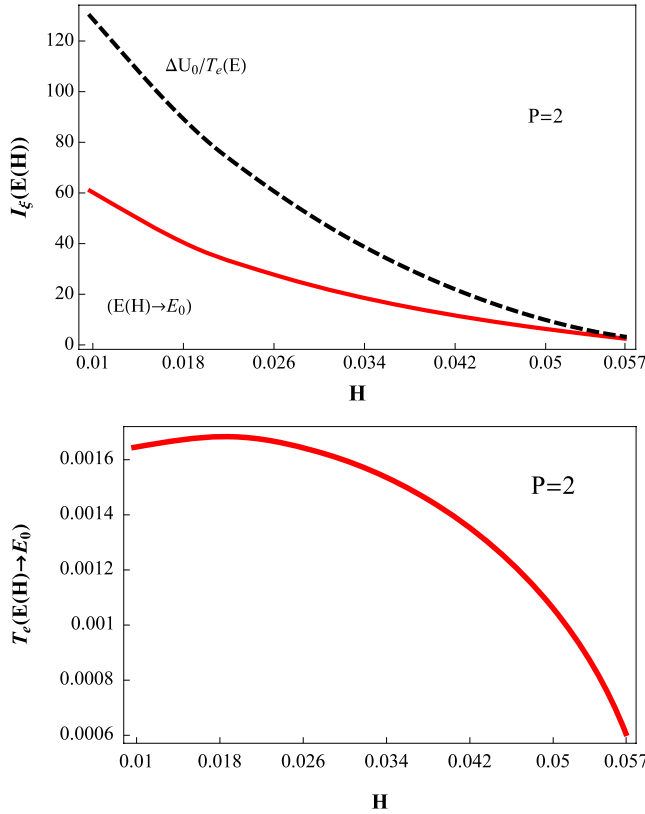


Figure 3. Escape exponent for instantons figure 2 with $P = 2$ and $H_{\text{ext}} = \mathbf{H}$ (upper panel). Temperature for the tunneling trajectories with $P = 2$ in figure 2 (upper panel). This temperature corresponds to each period marked for the blue points in figure 2.

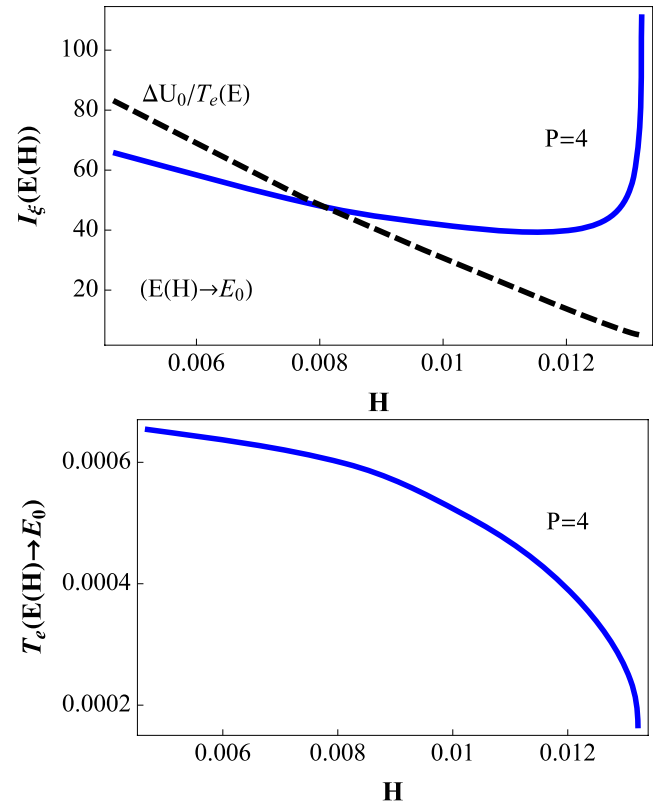


Figure 4. Escape exponent for instantons in figure 2 with $P = 4$ and $H_{\text{ext}} = \mathbf{H}$ (upper panel). Temperature for the tunneling trajectories with $P = 4$ in figure 2 (lower panel). This temperature corresponds to each period marked for the red points in figure 2.

by some approximation for $\cos \theta$ around $\pi/2$. This effective method allows tunneling in coherent minima for the canonical ϕ coordinate.

A second procedure that maps the system into a simpler one starts with the projection of equation (2) over the complete set of coherent states. Then a characteristic function $f_M(\mathbf{x}) = \sum_{M=-S}^S c_M \mathbf{x}^M$ (c_M being given constant coefficients) is proposed to rewrite the final projection as a Schrödinger wave equation. Afterwards, the function $f_M(\mathbf{x})$ should be restructured to include the symmetry $M \rightarrow -M$ by using some ansatz product (with $\mathbf{x} \rightarrow 1/\mathbf{x}$ dependence). Finally, this new function in the wave equation allows us to extract the final unidimensional effective potential $U_{\text{ef}}(\mathbf{x})$ [28, 29]. This mapping is more powerful for larger values of S , but is mathematically more involved because it generates a transcendental potential. In our case just quadratic anisotropy terms will be taken into account, since it is impossible to generate an adequate wavefunction equation to extract the effective potential unless $S \leq 10$.

In the procedure mentioned above the main objective is to reach the equation of motion for the instantons:

$$\frac{m(\phi)}{2} \dot{\phi}_\tau(\tau)^2 = V_{\text{ef}}(\phi(\tau)) - E(\tau_\xi) \quad (6)$$

$$\frac{m}{2} \dot{\mathbf{x}}_\tau(\tau)^2 = U_{\text{ef}}(\mathbf{x}(\tau)) - E(\tau_\xi). \quad (7)$$

These two equations are associated with each of the methods just described. After this, the period $\tau_\xi(E)$ can be calculated and used to evaluate I_ξ through

$$I_\xi = E\tau_\xi(E) + 2\sqrt{(2m')} \int_{q_1(E)}^{q_2(E)} dq \sqrt{V(q) - E} \quad (8)$$

where q is the imaginary tunneling coordinate, $q_{i=1,2}$ are the interception points between the inverted potential and the energy value, and m' is the mass given for the effective approach. At this point we propose an alternative equivalent integral relation, which can be obtained straightforwardly. Once the period of the instantons as a function of E is known, I_ξ is then:

$$I_\xi(T) = E(T)\tau_\xi(E) + \int_{E(T)}^{\Delta U_{\text{ef}}} dE' \tau_\xi(E'). \quad (9)$$

With equation (9) we can calculate the escape exponent of Γ and therefore the escape temperature $T_e(T)$. Moreover, the periodic behavior of the instantons can be used to understand the quantum to classical changeover, and the derivative of the Euclidean action gives us information about how sharp the transition is, i.e. from thermally assisted quantum tunneling to a classic thermally activated jump of the barrier [1, 27, 33]. In what follows we focus on the second mapping method along with the expression in equation (9). For $P = 2$ the effective

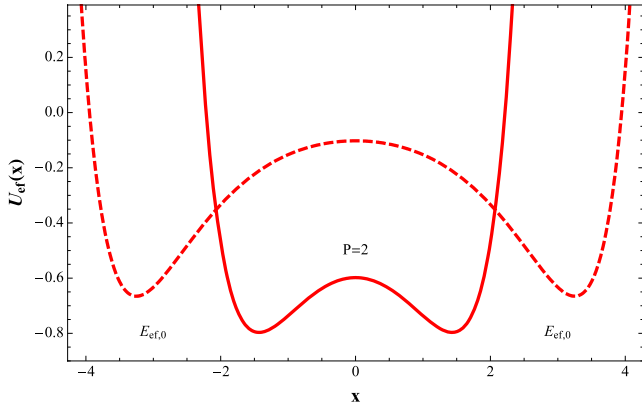


Figure 5. Effective potential equation (10) corresponding to two instantons; the dashed red line and continuous red line with $H_{\text{ext}} = (0.00975, 0.05697)$, respectively, in figure 1.

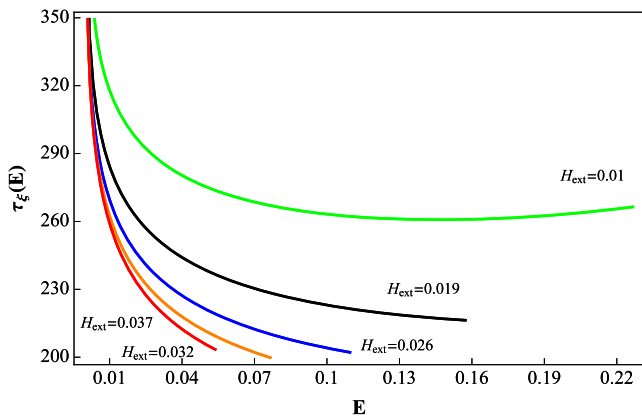


Figure 6. Period of the instantons as a function of energy E with equation (9) for the effective potential in equations (10) and (11). $S = 10$, $m = 166.7$ and H_{ext} for some illustrative cases.

particle potential in equation (7) is then given for

$$U_{\text{ef}}(\mathbf{x}) = \left(S + \frac{1}{2}\right)^2 \kappa_2 (h_x^2 \sinh^2 \mathbf{x} - 2h_x \cosh \mathbf{x}), \quad (10)$$

where the parameters are

$$m = \frac{1}{2\kappa_2} \quad \text{and} \quad h_x = \frac{H_{\text{ext}}}{(2S+1)\kappa_2}. \quad (11)$$

Figure 5 shows the effective potential corresponding to the initial Hamiltonian by using equations (10) and (11) with adequate parameters. In figure 6 the calculations for the period of the instantons for the effective potential in figure 5 are also shown.

3.2. Escape temperature and escape exponent for the effective potential

In this section we present results for the escape exponent and the escape temperature derived from the effective potential method. From the calculations with this method we can extract the instantons for the minimal energy used for all the magnetic fields, and the results for I_ξ versus H_{ext} in figure 7

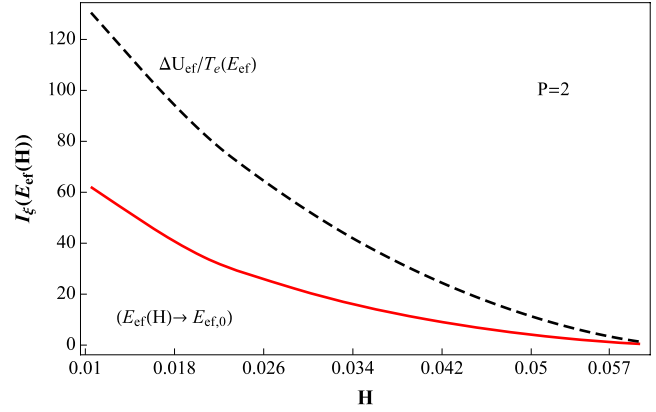


Figure 7. Escape exponent I_ξ versus $H_{\text{ext}} = \mathbf{H}$ using the periods of figure 6, for all considered magnetic fields. The dashed black line corresponds to Arrhenius-like thermal activation.

can be compared with the corresponding results shown in figure 3 where we used instanton solutions for the Euclidean action. Therefore, figure 7 shows results for the escape exponent $I_\xi(T)$ associated with the probability of magnetic quantum tunneling as a function of external field. The same figure also shows values for the exponent of the Arrhenius law $\Gamma \sim \exp(-\Delta U_{\text{ef}}/T)$, where ΔU_{ef} is the height of the effective barrier between coherent states. This illustrates how the behavior of the escape rate at a high external field for this effective potential is the same as the Arrhenius result with the effective temperature. Finally, in figure 8 we present the results for the escape temperature $T_e(T)$ characterizing the transition from the quantum to the classical regime as well as the results for the escape temperature as given by the Arrhenius law, i.e. $T_e(T) \approx T$.

4. Discussion

Our results illustrate how the inclusion of a metastable state between two coherent states affects the escape exponent and therefore Γ . The expression $\exp(-I_\xi/\hbar)$ evaluated on the escape exponent dominates (probabilistically) in the low magnetic field region compared with Arrhenius-like behavior. However, at higher external fields, H_{ext} , tunneling through coherent state no longer seems cheaper (energetically) and the magnetic moment can be easily trapped. In other words, at high magnetic fields the period of the instanton becomes longer as a consequence of classical force reduction in the vicinity of the metastable state.

For larger values of H_{ext} , the relation $\Delta U_o/\text{wide-barrier}$ is no longer big or similar and the oblate potential also gives rise to very long periods. The energy of the initial instantons when the field increases compared with ΔU_o is more comparable. This is similar to the case when the energy of the instantons is high even for fixed magnetic field; in this situation the instanton trajectory with enough energy can go through the metastable state and then to the other coherent state and so on, showing the contribution of another instanton's trajectories.

For the case of $P = 2$, and using the effective particle potential, we arrived at similar results to those of instanton

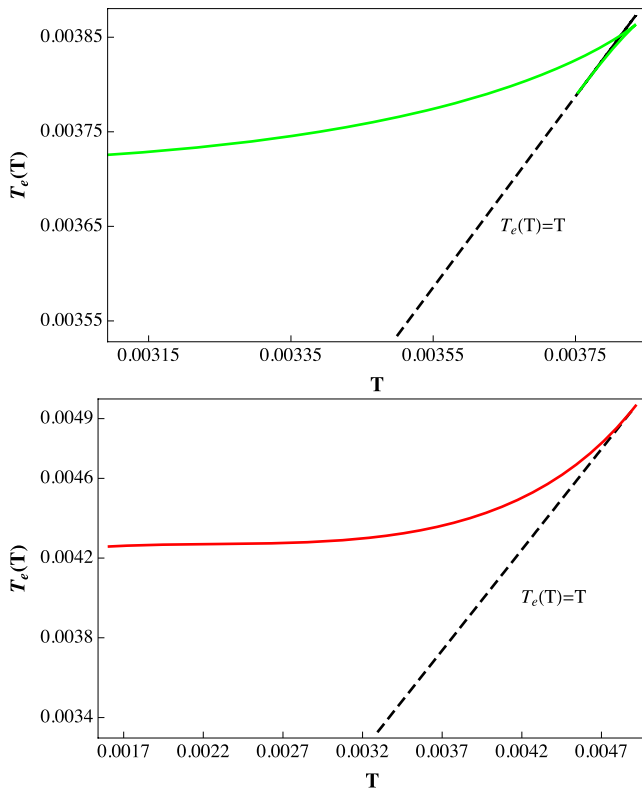


Figure 8. Escape temperature $T_e(T)$ for $H_{\text{ext}} = 0.01$ (upper panel) in green, and $H_{\text{ext}} = 0.037$ (lower panel) in red for the periods corresponding to the red and green lines shown in figure 6. The dashed-black line is the Arrhenius-like temperature $T_e(T) = T$.

solutions. Small discrepancies, however, are due to the different magnetic fields necessary to remove the barrier and to infinitesimal differences between the considered energy of the instanton in each case. The effective potential method includes, through the characteristic function, more configurations than the instanton method. This means that we have degrees of freedom with more information about the paths for the instantons. In this sense the effective potential can be used to estimate Γ for energies comparable with ΔU_{ef} . The escape temperature in figure 8 tells us that for low magnetic fields the first transition on the magnetic viscosity is likely, while the period of the instanton near to the top of the barrier increases as it moves closer the top, as can be seen in figure 6.

5. Conclusions

We have studied tunneling molecular magnets, within the giant spin approximation, between states separated by an intermediate metastable state. The presence of such a state is ensured by the modification of the anisotropy contributions on the magnetic Hamiltonian. We calculated the escape rate for tunneling under Zeeman interaction transverse to the anisotropy axis using the instanton formalism, and by taking into account not only the quadratic anisotropy term but also the contribution of fourth-order terms. Fourth-order terms add a kink to the instanton solution, making its period longer at higher external fields. This has the consequence of stabilizing

the magnetic moment of the coherent states and therefore reducing the tunneling amplitude among them.

Moreover, for $P = 2$ we use a mapping technique for the effective action, obtaining a unidimensional particle-like equation of motion. Then we find the escape exponent I_{ξ} and the escape temperature T_e characterizing the crossing from thermally assisted quantum tunneling to classical thermal activation. The results fully agree with the instanton description of the same problem.

New experimental and theoretical developments of MNMs reveal the importance of different orders of anisotropy constants [13, 31], thus opening up the possibility of using the simplified description presented here.

Acknowledgments

This work was supported by the PIIC 2009 of the DGIP of the Universidad Técnica Federico Santa María. ASN's work was partially funded by Proyecto de Iniciación en investigación Fondecyt 11070008 and Proyecto Bicentenario de Ciencia y Tecnología, ACT027. PV acknowledges Fondecyt grant 1070224. The authors also acknowledge partial funds from Núcleo Científico Milenio 'Magnetismo Básico y Aplicado' P06022-F.

References

- [1] Chudnovsky E M and Tejada J 1998 *Macroscopic Quantum Tunneling of the Magnetic Moment* (Cambridge: Cambridge University Press)
- [2] Gunther L and Barbara B 1994 *QMT' 94: Quantum Tunneling of Magnetization*
- [3] Sessoli R, Gatteschi D, Caneschi A and Novak M A 1993 *Nature* **365** 141
- [4] Chudnovsky E M and Gunther L 1988 *Phys. Rev. B* **37** 9455
- [5] Barbara B and Chudnovsky E M 1990 *Phys. Lett. A* **145** 205
- [6] Chudnovsky E M, Iglesias O and Stamp P C E 1992 *Phys. Rev. B* **46** 5392
- [7] Tejada J, Zhang X X and Chudnovsky E M 1993 *Phys. Rev. B* **47** 14977
- [8] Chudnovsky E M 1995 *J. Magn. Magn. Mater.* **140** 1821
- [9] Friedman J R, Sarachik M P, Tejada J and Ziolo R 1996 *Phys. Rev. Lett.* **76** 3830
- [10] Tejada J, Zhang X X, del Barco E, Hernández J M and Chudnovsky E M 1997 *Phys. Rev. Lett.* **79** 1754
- [11] Wernsdorfer W, Clérac R, Coulon C, Lecren L and Miyasaka H 2005 *Phys. Rev. Lett.* **95** 237203
- [12] Sangregorio C, Ohm T, Paulsen C, Sessoli R and Gatteschi D 1997 *Phys. Rev. Lett.* **78** 4645
- [13] Brooke J, Rosenbaum T F and Aepli G 2001 *Nature* **413** 610
- [14] Wernsdorfer W and Sessoli R 1999 *Science* **284** 133
- [15] Wernsdorfer W, Bhaduri S, Boskovic C, Christou G and Hendrickson D N 2002 *Phys. Rev. B* **65** 180403
- [16] Barbara B et al 1995 *J. Magn. Magn. Mater.* **140** 1825
- [17] Leuenberger M N and Loss D 2000 *Phys. Rev. B* **61** 1286
- [18] Garg A and Kim G-H 1992 *Phys. Rev. B* **45** 12921
- [19] Keçecioglu E and Garg A 2002 *Phys. Rev. Lett.* **88** 237205
- [20] Luis F, Bartolomé J and Fernández J F 1998 *Phys. Rev. B* **57** 505
- [21] Yang J-S and Chang C-R 2005 *J. Magn. Magn. Mater.* **287** 303
- [22] Li Y 2006 *J. Magn. Magn. Mater.* **303** 243
- [23] Kak M, Stephan R, Mehdaoui A, Berling D, Bolmont D, Gewinner G and Wetzel P 2004 *Surf. Sci.* **566** 278

- [23] Liang J-Q, Zhang Y-B, Müller-Kirsten H J W, Zhou J-G, Zimmerschied F and Pu F C 1998 *Phys. Rev. B* **57** 529
- [24] Liang J-Q, Müller-Kirste H J W, Park D K and Zimmerschied F 1998 *Phys. Rev. Lett.* **81** 216
- [25] Chen Z-D 2002 *Phys. Rev. B* **65** 085313
- [26] Garanin D A and Chudnovsky E M 1997 *Phys. Rev. B* **56** 11102
- [27] Chudnovsky E M and Garanin D A 1997 *Phys. Rev. Lett.* **79** 4469
- [28] Scharf G, Wreszinski W F and Van Hemmen J L 1987 *J. Phys. A: Math. Gen.* **20** 4309
- [29] Zaslavkii O B 1990 *Phys. Rev. B* **42** 992
- [30] Carretta S, Liviotti E, Magnani N, Santini P and Amoretti G 2004 *Phys. Rev. Lett.* **92** 207205
- [31] Carretta S *et al* 2008 *Phys. Rev. Lett.* **100** 157203
- [32] Hannggi P, Talkner P and Borkovec M 1990 *Rev. Mod. Phys.* **62** 251
- [33] Chudnovsky E M 1992 *Phys. Rev. A* **46** 8011
- [34] Affleck I 1981 *Phys. Rev. Lett.* **46** 388